Published in final edited form as:
Cancer Res. 2011 March 15; 71(6): 2286–2297. doi:10.1158/0008-5472.CAN-10-3367.

MYC Phosphorylation, Activation, and Tumorigenic Potential in Hepatocellular Carcinoma are Regulated by HMG-CoA Reductase

Zhongwei Cao[1,*], **Hua Fan-Minogue**[2,*], **David I. Bellovin**[1,*], **Aleksey Yevtodiyenko**[1,*], **Julia Arzeno**[1], **Qiwei Yang**[1], **Sanjiv Sam Gambhir**[2], and **Dean W. Felsher**[1,†]

[1] Division of Medical Oncology, Departments of Medicine and Pathology, Molecular Imaging Program at Stanford, Stanford University, Stanford, CA 94305-5151, USA

[2] Departments of Radiology, Bioengineering & Materials Sciences and Engineering, Molecular Imaging Program at Stanford, Stanford University, Stanford, CA 94305-5151, USA

Abstract

MYC is a potential target for many cancers but is not amenable to existing pharmacological approaches. Inhibition of HMG-CoA reductase by statins has shown potential efficacy against a number of cancers. Here, we demonstrate that inhibition of HMG-CoA reductase by atorvastatin blocks both MYC phosphorylation and activation, suppressing tumor initiation and growth *in vivo* in a transgenic model of MYC-induced HCC as well as in human HCC-derived cell lines. To confirm specificity, we show that the anti-tumor effects of atorvastatin are blocked by co-treatment with the HMG-CoA reductase product, Mevalonate. Moreover, by using a novel molecular imaging sensor, we confirm that inhibition of HMG-CoA reductase blocks MYC phosphorylation *in vivo*. Importantly, the introduction of phosphorylation mutants of MYC at Ser62 or Thr58 into tumors blocks their sensitivity to inhibition of HMG-CoA reductase. Finally, we demonstrate that inhibition of HMG-CoA reductase suppresses MYC phosphorylation through Rac GTPase. Therefore, HMG-CoA reductase is a critical regulator of MYC phosphorylation, activation, and tumorigenic properties. The inhibition of HMG-CoA reductase may be a useful target for the treatment of MYC-associated HCC as well as other tumors.

Keywords

MYC; HMG-CoA Reductase; Hepatocellular Carcinoma

Introduction

Hepatocellular carcinoma (HCC) is one of the most common and generally incurable malignancies with an estimated 9% 5-year survival rate (1). Hepatocellular carcinogenesis is strongly associated with hepatitis B and C virus (HBV and HCV) infection, as well as other pathological conditions resulting in liver regeneration (2), which in turn facilitates the activation of specific oncogenes, most notably MYC (3). Thus, targeted inactivation of MYC may be an effective therapy for HCC (4–6). Indeed, we have reported recently that the

[†]Address correspondence to: Dean W. Felsher, MD PhD, Stanford University School of Medicine, 269 Campus Drive, CCSR 1105, Stanford, CA 94305-5151, dfelsher@stanford.edu.
[*]Authors contributed equally to this work

Conflicts of Interest: None

conditional inactivation of MYC can be sufficient to induce sustained regression of HCC (7). However, there is no existing therapy for patients that targets MYC for the treatment of any cancer.

The MYC proto-oncogene family is comprised of c-MYC, N-MYC, and L-MYC and has been shown to impact almost every aspect of tumorigenesis, including promoting unrestricted cell proliferation, inhibiting cell differentiation, reducing cell adhesion, and enhancing metastasis, genomic instability and angiogenesis (8,9). MYC functions as an oncogene upon over-expression, either due to increased expression of the *myc* gene or by increased stability of the MYC protein. MYC protein stability is regulated through the ubiquitin/26S proteasome pathway and the sequential phosphorylation of MYC at Serine 62 (S62) and Threonine 58 (T58) (10). The phosphorylation of S62 is mediated by the MAPK/ERK pathway and contributes to the stabilization of MYC. Subsequent phosphorylation of T58, mediated by GSK3β, promotes ubiquitin-dependent MYC degradation once S62 is dephosphorylated (11–13). Mutations in these phosphorylation sites that stabilize MYC protein have been identified in human cancers, thereby highlighting the importance of S62 and T58 phosphorylation as regulators of MYC in tumorigenesis (14,15). Hence, targeting MYC phosphorylation could be useful as an anti-cancer therapy.

The enzyme 3-hydroxy-3-methylglutaryl-coenzyme A reductase (HMG-CoA reductase) controls the rate-limiting step in the mevalonate pathway that is essential for cholesterol biosynthesis (16). Statins were initially utilized to inhibit HMG-CoA reductase as a means to reduce the serum cholesterol level (16). However, many studies have shown that inhibition of HMG-CoA reductase also has anti-tumor efficacy both *in vitro* and *in vivo* in multiple tumor types (17–20), including colorectal cancer (21,22), breast cancer (23), melanoma (24), and lymphoma (25). Statins have been suggested to block tumor cell growth through the inhibition of proliferation and angiogenesis, induction of apoptosis, and repression of tumor metastasis (26).

Statins may mediate their anti-cancer properties through inhibition of the synthesis of lipid isoprenoid intermediates that are produced downstream of the mevalonate pathway, including farnesyl pyrophosphate (FPP) and geranylgeranyl pyrophosphate (GGPP) (19). Generally, FPP activates the Ras GTPase family while GGPP activates the Rho/Rac family by prenylating and anchoring them on the cell membrane (27). Both Ras (12,27) and Rho/Rac family members (28) are required to phosphorylate MYC. Hence, we speculated, that by inhibiting these pathways, statins might therefore block MYC activation.

Here we show that the inhibition of HMG-CoA reductase by atorvastatin (AT) inhibits MYC phosphorylation and activation and thereby blocks MYC-induced HCC onset and tumor maintenance. Moreover, by using a novel molecular imaging sensor that noninvasively detects c-Myc phosphorylation, we found, both *in vitro* in human HCC cells and *in vivo* in mice, that AT inhibits MYC phosphorylation. Furthermore, the introduction of mutant MYC alleles that cannot be phosphorylated on S62 or T58 prevented AT from inhibiting the *in vivo* tumor growth of HCC. Finally, we provide evidence suggesting that AT may mediate these effects on MYC phosphorylation and activation by inhibiting Rac GTPase. Therefore, HMG-CoA reductase appears to be a critical regulator of MYC activation and may have potent activity against MYC-induced cancers.

Materials and Methods

Antibodies

The antibody to Ki67 was obtained from BD Biosciences (San Jose, CA); c-MYC, Cdk4, E2F1, and Rac1 antibodies were obtained from Santa Cruz Biotechnology (Santa Cruz, CA);

phospho-c-MYC was obtained from Cell Signaling Technology (Danvers, MA); antibodies to Tubulin and HA were from Sigma-Aldrich (St Louis, MO). Horseradishperoxidase-conjugated sheep anti-mouse IgG and sheep anti-rabbit IgG were obtained from GE Healthcare (Little Chalfond Buckinghamshire, UK) and Biotinylated anti-mouse IgG was from BD Biosciences.

Cell Lines

The Huh7 and HepG2 cell lines were obtained from the ATCC originally characterized by DNA profile and cytogenetic analysis and were passaged for less than 6 months *in vitro*.

Transgenic mice

The Tet-system was used previously to generate transgenic mice that conditionally express human c-MYC cDNA in hepatocytes, as described (7). MYC expression was induced by removing doxycycline (Dox, 100μg/ml) from the drinking water of mice. All animals were maintained and treated in accordance with the policies of Stanford University.

Atorvastatin treatment

Atorvastatin (AT, prescription formulation; Pfizer Inc, New York, NY) was resuspended in PBS. AT was administered orally in 100mg/kg doses with or without 20mg/kg mevalonate (MV) 3 times a week using 20-mm feeding needles (Popper and Sons, New Hyde Park, NY). PBS was administered as a negative control.

Purified AT (Sequoia Research Products, Pangbourne, United Kingdom) resuspended in 100% DMSO was used for *in vitro* studies.

Histology and immunohistochemistry

Tissues were fixed in 10% buffered formalin and embedded in paraffin. Sections of 5 μm were stained with hematoxylin-eosin (H&E), or analyzed by immunohistochemistry using the antibody to Ki67. DAB (Vector Laboratories, Redwood City, CA) was used to achieve color development.

Proliferation assay

Cells were seeded in 24-well plates (5000 cells per well) and incubated overnight. Next, cells were treated with PBS, AT (0.5, 1.0, 2.5, 5.0, 10, or 25 μM), 10 or 25μM AT and 100μM MV, 10 or 25μM AT and 10μM FPP, or 10 or 25μM AT and 10μM GGPP for 96 hours. Cell proliferation was evaluated using the3-(4, 5- dimethylthiazo-2-yl)-2, 5-diphenyltetrazolium bromide(MTT) assay. Data were from six replicated experiments.

Quantitative real-time polymerase chain reaction (qPCR)

HCC cells were treated with PBS, 20 ng/mL Dox, 10μM AT, or 10μM AT and 100μM MV for 24 hours. Total mRNA from HCC cells was extracted and purified using the RNeasy Mini Kit from Qiagen (Austin, TX) and quantified by spectrophotometer (Beckman Coulter, Fullerton, CA). cDNA was reverse-transcribed from 2μg of total mRNA using oligo-d(T) primers. Real-time PCR analysis was performed in an ABI PRIZM analyzer (Applied Biosystems, Foster City, CA).

Cell membrane fractionation and protein isolation

Cells ($2x10^8$) were washed 3 times with PBS and extracted in lysis buffer (50 mM Tris, 50 mM NaCl, 2 mM EDTA, 1 mM $MgCl_2$, 10 mM NaF, 1 mM DTT, pH 7.4). Lysates were centrifuged at 36,000 rpm for 40 minutes using Beckman L8-70M ultracentrifuge. The

membrane pellet was solubilized in immunoprecipitation buffer (0.15 M NaCl, 1% Triton X-100, 0.1% SDS, 0.5% sodium deoxycholate, 10 mM Tris-HCl, pH 7.4) and incubated at 4°C for 30 minutes. The solution was centrifuged at 15,000 rpm for 10 minutes, and the supernatant was collected as the membrane protein fraction.

Viral infection

Ad-c-MYC^{WT}, Ad-c-MYC^{S62A}, and Ad-c-MYC^{T58A} viruses were kindly provided as a gift from Dr Rosalie C. Sears (Oregon Health & Science University, Portland, OR). Briefly, Ad-c-MYC^{WT}, Ad-c-MYC^{S62A}, and Ad-c-MYC^{T58A} adenovirus were cloned by inserting c-MYC^{WT} (Ad-c-MYC^{WT}), c-MYC^{S62A} (Ad-c-MYC^{S62A}) and c-MYC^{T58A} (Ad-c-MYC^{T58A}) cDNA into the pADEasy-1 backbone (Stratagene, La Jolla, CA). Transplanted tumor cells were infected as previously described (29). Briefly, SCID mice were injected with hepatocellular carcinoma cells isolated from LAP-tTA/TRE-MYC transgenic mice. Tumor masses were injected in three sites with Ad-c-MYC^{WT} or Ad-c-MYC^{T58A} once every week. Successful infection was confirmed by GFP co-expression in tumors (Supplementary information, Fig. S9). Mice were treated with 100μg/mL Dox to inactivate transgenic MYC expression. Tumor growth was measured using calipers three times a week for three weeks after viral injection.

Immunoprecipitation and immunoblotting

Cells were lysed in immunoprecipitation buffer (0.15 M NaCl, 1% Triton X-100, 0.1% SDS, 0.5% sodium deoxycholate, 10 mM Tris-HCl, pH 7.4) and cleared lysates were immunoprecipitated with 2μg HA antibody. The precipitated proteins were resolved by sodium dodecyl sulfate-polyacrylamide gel electrophoresis (SDS-PAGE), transferred to nitrocellulose, and blotted with the antibodies indicated in the figures. Total MYC and phospho-MYC level were detected by immunoblotting, and their optical density (OD) was measured and normalized to actin band OD. The MYC phosphorylation level was determined by the ratio between phospho-MYC and total MYC.

Molecular imaging of c-Myc phosphorylation

A bioluminescent sensor system that can noninvasively detect c-Myc phosphorylation was utilized to detect the AT inhibitory effect in intact cells and living mice. The sensor system utilizes the fact that S62 phosphorylation of c-Myc is required for its interaction with GSK3β and detects the protein interaction between GSK3β and c-Myc to indirectly report the c-Myc phosphorylation using a split Firefly luciferase (FL) complementation system (30). Specific GSK3β and c-Myc fragments are fused with the inactive C-terminal and N-terminal fragment of the split FL respectively (GSK35-433-CFL/NFL-c-Myc). Phosphorylation-induced interaction between GSK3β and c-Myc brings the two split fragments into close proximity and recovery of the luciferase activity.

The sensor system has been validated both in intact cells and mouse xenograft model, which is described in an independent manuscript (31). For *in vitro* imaging, the sensor plasmids were transiently transfected into HuH7 and HepG2 cells using Superfect (Qiagen) and Lipofectamine2000 (Invitrogen) reagent respectively. Renilla luciferase gene was co-transfected for the control of the transfection efficiency. 24hrs after transfection, cells were treated with AT with different concentration as indicated for 18hrs. Bioluminescent imaging (BLI) was performed in IVIS 50 (Caliper life science, Hopkinton, MA) after adding 45μg/ml D-Luciferin (Promega) to the cells. Cells were lysed for RL assay (Promega) and western blot analysis after imaging. For *in vivo* liver tumor imaging, we used a hydrodynamic injection method as previously described (32). Briefly, 2ml of saline solution containing 25μg of the MYC sensor plasmid with CMV promoter was injected into the tail vein within 8 seconds. Mice were imaged in IVIS 200 22hrs after injection based on time course of the

sensor expression as determined in control experiments (Supplementary information, Fig. S6 and S7).

Results

Inhibition of HMG-CoA reductase by atorvastatin suppresses MYC-induced HCC

The effects of inhibition of HMG-CoA reductase were examined on HCC growth *in vitro* and *in vivo* by administering atorvastatin (AT) to multiple HCC tumor cell lines derived from the LAP-tTA/TRE-MYC transgenic mice, a previously described conditional transgenic model of MYC-induced HCC using the Tet-system (7), in addition to human HCC cell lines. The murine cell lines were all generated from HCC isolated from dual transgenic animals. These cell lines are dependent upon high levels of human MYC expression, which can be inactivated upon treatment with doxycycline (Dox). Hence, in these transgenic tumor-derived cell lines, as a positive control for MYC inactivation, we used Dox to induce the suppression of transgenic MYC. Doses of AT used for our experiments were comparable to previously published studies (33,34). Moreover, as control for nonspecific effects of statins, we confirmed that effects were reversed with co-treatment with the enzyme product of HMG-CoA reductase, mevalonate (MV). Note that because of marked differences in the pharmacokinetics between mouse and human, AT doses in mice are approximately 50-fold higher than the pharmacologically equivalent dose in humans (35,36).

First, AT inhibited the *in vitro* proliferation of the MYC-induced HCC murine cell line 3-4 as measured by the MTT assay (Fig. 1a and Supplementary information, Fig. S2a; 75% decrease at 10μM and 92% decrease at 25μM AT at 96 hours of AT treatment, $p<0.0001$ each). Also, AT decreased the number of cells in S-phase and G2/M from 38% to 26% as assessed by propidium iodide staining (Fig. 1b, $p=0.01$), and reduced Ki67 immunofluorescence from 81.4% to 31.2% following 48 hours of 10μM AT treatment (Fig. 1c, $p<0.0001$). Importantly, the effects of AT on proliferation and cell cycle arrest were rescued by co-treatment with MV, the immediate downstream target of HMG-CoA reductase (Fig. 1a–c), confirming these effects are specific to inhibition of the cholesterol biosynthesis pathway. Moreover, AT was found to similarly inhibit proliferation and induce cell cycle arrest and apoptosis in two independently derived murine HCC cell lines, EC4 and HCC 4–4, in a dose-dependent manner (Supplementary information, Fig. S1–S3). Thus, AT inhibits proliferation and induces apoptosis of murine HCC tumor cells *in vitro*.

Second, AT inhibited the growth of the murine HCC 3–4 cell line transplanted into syngeneic mice by up to 80% compared with treatment by PBS or AT and MV (Fig. 1d, e, $p=0.0003$). Note, that FVB/N mice treated with 100mg/kg AT did not exhibit any general toxicity and, in particular, had normal liver histology and serum bilirubin levels, demonstrating the clinical effects are not secondary nonspecific hepatotoxicity (Supplementary information, Fig. S4). Therefore, inhibition of HMG-CoA reductase by AT has potent *in vivo* anti-tumor activity against murine MYC-induced HCC.

Third, we interrogated the ability of AT to suppress growth in Huh7 cells, a human HCC cell line. AT blocked the *in vitro* growth of Huh7 cells over a 96-hour time course (Fig. 2a and Supplementary information, Fig. S2b; 69% decrease at 10μM and 86% decrease at 25μM AT, $p<0.0001$ each) while inhibiting cell cycle progression (Fig. 2b; 75% reduction in S-phase, $p=0.003$) and reducing Ki67 positivity (Fig. 2c; 58% reduction, $p<0.0001$) following 48 hours of 10μM AT treatment. Moreover, AT suppressed the *in vivo* growth of Huh7 cells (Fig. 2d; PBS *versus* AT, $p=0.03$; AT *versus* AT+MV, $p=0.04$; PBS *versus* AT +MV, $p=0.8$). Co-treatment with MV blocked the effects of statin treatment, confirming that

the inhibition of human HCC by AT is specific to the suppression of HMG-CoA reductase (Fig. 2a–d).

Finally, we evaluated the ability of HMG-CoA reductase inhibition to block the initiation of MYC-induced HCC growth *in vivo* in the LAP-tTA/TRE-MYC transgenic mice treated with PBS, AT, or AT with MV (Fig. 3a, left). Treatment with 100mg/kg AT *versus* PBS significantly delayed tumor onset and increased survival (Fig. 3a; median survival increased from 80 days to 147 days, $p<0.005$). Importantly, MV treatment prevented AT from inhibiting tumorigenesis (Fig. 3a). Gross pathology revealed that AT markedly reduced the size and frequency of tumor nodules (Fig. 3b, Left). H&E staining revealed histologically normal liver tissue in AT-treated mice, suggesting a robust inhibition of disease onset (Fig. 3b, Middle). AT-treat animals also exhibited evidence of inhibited cell proliferation, as indicated by reduced Ki67 staining compared to PBS-treated mice (Fig. 3b, Right; 8 ± 3 positive cells *versus* 422 ± 23 positive cells per field, $p<0.02$). Hence, inhibition of HMG-CoA reductase by AT is potent at inhibiting MYC-induced liver tumorigenesis.

Inhibition of HMG-CoA reductase suppresses MYC phosphorylation, stability, and transactivation

MYC activation has been shown to be regulated by phosphorylation (12). Thus, we considered that AT might exert its anti-neoplastic effects by inhibiting MYC phosphorylation. Indeed, AT, but not AT with MV, was found to induce a dose-dependent down-regulation of MYC phosphorylation *in vitro* upon 24 hours treatment (Fig. 4a; 29% reduction at 0.5μM, 34% at 1.0μM, 79% at 2.5μM, 83% at 5.0μM, 94% at 10 μM, and 97% at 25μM AT; $p=0.004$) as well as *in vivo* (Fig. 4b; 93% reduction). Moreover, AT blocked MYC phosphorylation in MYC-induced murine lymphoma, osteosarcoma and lung cancer, as well as in human breast cancer cell lines (data not shown). In turn, the de-phosphorylation was associated with a reduction in MYC protein levels *in vitro* (Fig. 4a; 17% reduction at 0.5μM, 40% at 1.0μM, 9% at 2.5μM, 41% at 5.0μM 69% at 10μM and 91% at 25μM AT, $p=0.002$) and *in vivo* (Fig. 4b; 57% reduction, $p=0.04$). Importantly, the inhibition of MYC phosphorylation by AT not only reduced MYC levels but appeared to dramatically inhibit MYC transcriptional activation as illustrated by the reduced mRNA expression of canonical target genes ODC and nucleolin, both in murine (Fig. 4c; 72% reduction for ODC, $p=0.003$; 76% reduction for nucleolin, $p=0.03$) and in human HCC upon 24 hours of 10μM AT treatment (Fig. 4d; 64% reduction for ODC, $p=0.016$; 59% reduction for nucleolin, $p=0.008$; Supplementary information, Fig. S8b). Thus, the inhibition of HMG-CoA reductase blocks MYC phosphorylation, reduces MYC protein levels, and inhibits MYC transactivation.

Noninvasive molecular imaging to measure *in vivo* MYC phosphorylation

To evaluate the effects of inhibition of HMG-CoA reductase on MYC phosphorylation *in situ* in a living host, we utilized a novel molecular imaging sensor system (31). The sensor system consists of two parts: 1) a peptide corresponding to the phospho-regulated domain of MYC fused to the N-terminal domain of Firefly luciferase (FL) and 2) the C-terminal domain of FL fused to a peptide fragment of GSK3β that recognizes phospho-MYC (Fig. 5a). When co-expressed in an intact cell, MYC phosphorylation can be detected via interaction between the MYC and GSK3β peptides, thereby localizing the N- and C-termini of FL in close proximity, conferring luciferase activity. Renilla luciferase (RL) is co-transfected as a control for transfection efficiency. The full-length Firefly luciferase (FL) was also transfected independently into these cells as a control for the direct effect of AT on luciferase activity. We confirmed that this imaging method could detect the dose dependent reduction of c-Myc phosphorylation in human Huh7 and HepG2 cells upon 18hrs of AT treatment (Fig. 6b,c and Supplementary information, Fig. S5, *p<0.0001).*

Next, this imaging sensor was used to monitor MYC phosphorylation *in vivo*. The sensor system was introduced in liver cells of LAP-tTA/TRE-MYC mice by hydrodynamic injection. Two groups of transgenic mice (n=3 each) had MYC activated at the same time and were treated with either AT or PBS. The MYC sensor was imaged at day 0 and day 15 post-treatment. The PBS-treated group showed no significant change of the sensor signal, while the AT-treated group showed 72% reduction of the sensor signal at day 15 of treatment (Fig. 5d,e; AT-treated mice day 0 *versus* day 15, *p=0.038*; PBS-treated day 0 *versus* day 15, *p=0.638*). Notably, AT-mediated inhibition of MYC phosphorylation *in vivo* was associated with a 44% and 56% down-regulation in the expression of downstream target genes, E2F1 and Cdk4 (Supplementary information, Fig. S8a), further demonstrating the inhibition of MYC activity. Hence, a novel imaging sensor was used to show that the inhibition of HMG-CoA reductase by AT inhibits MYC phosphorylation *in vivo*.

MYC phospho-mutants confer resistance to the inhibition of HMG-CoA Reductase

To examine if inhibition of MYC phosphorylation mediates the anti-cancer effect of AT, we introduced phospho-mutants of MYC into HCC tumor cell lines. First, recombinant adenovirus was used to express MYC that is mutated with either an Alanine substitution at either S62 or T58 (Ad-MYC^{S62A} and Ad-MYC^{T58A}) and hence cannot be regulated by phosphorylation at these sites (37). AT treatment at 10μM for 24 hours dramatically suppressed WT MYC but failed to significantly inhibit protein levels of either S62A MYC or T58A MYC (Fig. 6a; MYC^{S62A} *versus* MYC^{S62A}+AT, p=0.09; MYC^{T58A} *versus* MYC^{T58A}+AT, p=0.06). Thus, we concluded that phospho-regulation through either S62 or T58 is necessary for AT to suppress MYC expression.

Using an antibody specific for phospho-S62 and -T58, we show that AT inhibits phosphorylation in T58A MYC similar to wild-type MYC (Fig. 6a, 62% reduction for MYC^{WT}, p=0.01; 68% reduction for MYC^{T58A}, p=0.008). These data show that the reduction of phospho-MYC by AT appears to occur by preventing S62 phosphorylation. However, the reduction of total MYC protein cannot occur without T58 phosphorylation. In addition, HCC cells expressing the S62A MYC mutant were less sensitive whereas cells expressing T58A MYC were completely insensitive to the inhibition of proliferation upon AT treatment (Fig. 6b, 26% reduction for WT, p<0.001; 17% reduction for S62, p<0.0001; no reduction for T58, p=0.8). Thus, inhibition of HMG Co-A reductase suppresses MYC activation in a phosphorylation-dependent manner.

Next, we investigated whether the MYC phospho-mutants could suppress the ability of the inhibition of HMG Co-A reductase to block HCC tumor growth *in vivo*. Syngeneic hosts were transplanted with MYC-induced HCC cells that were then injected with Ad-MYC^{WT}, Ad-MYC^{S62A}, or Ad-MYC^{T58A}. Tumor growth was monitored in response to AT, PBS, or AT with MV treatment (Fig. 6c). The adenoviral delivery of the MYC phospho-mutants was confirmed by co-expression of GFP (Supplementary information, Fig. S9). To suppress the conditional transgenic MYC expression, mice were treated with doxycycline, thereby resulting in the effective knock-in of the Ad-MYC^{WT}, Ad-MYC^{S62A}, or Ad-MYC^{T58A} constructs into the HCC cells. HCC growth upon injection of Ad-MYC^{WT} showed 66% inhibition by 100mg/kg AT but not by PBS or AT and MV treatment (Fig. 6d, Left, PBS *versus* AT, p=0.01; AT *versus* AT+MV, p=0.007). However, HCC tumors that were injected with Ad-MYC^{S62A} exhibited only 44% inhibition of tumor growth upon treatment with AT (Fig. 6d, Middle, PBS *versus* AT, p=0.02; AT *versus* AT+MV, p=0.03). Tumors that were injected with Ad-MYC^{T58A} showed complete rescue from sensitivity to AT treatment (Fig. 6d, Right, PBS *versus* AT, p=0.56; AT *versus* AT+MV, p=0.03). Therefore, MYC phosphorylation is necessary for AT to inhibit MYC-induced HCC tumor growth.

Inhibition of HMG-CoA reductase may block MYC activity through Rac GTPase

We examined if the inhibition of HMG-CoA reductase blocks MYC activation through Rac GTPases. Statins block production of the isoprenoids farnesyl pyrophosphate and geranylgeranyl pyrophosphate (23,38,39). FPP prenylates the Ras, Rheb, and PTP4A3 family while GGPP prenylates the Rac, Rho, and Cdc42 family of small GTPases (16). Previous studies suggest that Ras and Rac/Rho families of GTPases may contribute to the regulation of MYC phosphorylation (25). Thus, the inhibition of HMG-CoA reductase is likely to prevent MYC phosphorylation through these GTPases

To explore the role of GTPases in mediating inhibition of MYC phosphorylation, we performed several experiments. First, to control GTPase activity, we supplemented growth media with either FPP or GGPP before 96hrs AT treatment of MYC-induced murine HCC cells *in vitro*. Both MV and GGPP restored HCC cell proliferation to levels similar to DMSO controls (Fig. 7a; DMSO *versus* AT+MV, p=0.07; DMSO *versus* GGPP, p=0.053), whereas FPP demonstrated significantly less reduction in AT-mediated growth inhibition (DMSO *versus* FPP, p<0.002). Similarly, in Huh7 cells, GGPP was more potent than FPP in abrogating the effect of 96hrs of 10μM AT on proliferation (Fig. 7b; 16% reduction for DMSO *versus* AT+MV, p <0.01; 16% reduction for DMSO *versus* GGPP, p<0.01; 32% reduction for DMSO *versus* FPP, p<0.001). In addition, GGPP was more efficient in rescuing the transcription of multiple MYC target genes than FPP, including Cdk4 and E2F1, following 24 hours of 10μM AT treatment (Supplementary information, Fig. S10, 40–45% reduction for FPP, p<0.001; 25–60% increase for GGPP, p<0.03). MYC phosphorylation was restored to levels similar to PBS-treated controls when media containing 10μM AT was supplemented with GGPP but not with FPP (Fig. 7c; 76% reduction for FPP, p=0.001; 21% reduction for GGPP, p=0.02). Therefore, inhibition of HMG-CoA reductase appears to inactivate MYC through the inhibition of the Rho/Rac pathway.

Finally, we examined the potential role of the Rac/Rho/Cdc42 pathway as a mechanism by which AT suppresses MYC activation. First, we investigated if AT was influencing the membrane localization of Rac1. Indeed, 24-hour treatment with 10μM AT resulted in the delocalization of Rac1 from the plasma membrane (Fig. 7d; 83% reduction for AT, p<0.001). As a control, we showed that treatment with MV blocked these effects, as did treatment with GGPP (Fig. 7d; no change for PBS *versus* AT+MV, p=0.08; 37% increase for PBS *versus* GGPP, p<0.03). Notably, AT had little effect on Ras localization (data not shown). Second, using a Rac pull-down assay, 24 hours of 10 μM AT treatment was shown to reduce Rac1 activity by 77% (Fig. 7e). Thus, the inhibition of HMG-CoA reductase by AT appears to suppress activation of the Rac pathway, suggesting that AT in blocks MYC phosphorylation and activation via inhibition of Rac.

Discussion

Here, we demonstrate that MYC phosphorylation, activation, and thereby tumorigenic potential are regulated by HMG-CoA reductase. In particular, the inhibition of HMG-CoA reductase by statins suppresses MYC phosphorylation and activation. The consequences of these effects on MYC include preventing HCC initiation as well as inhibiting the *in vivo* growth of established murine and human HCC tumors. Moreover, statins, by blocking HMG-CoA reductase, inhibit GTPase activity, thereby resulting in MYC dephosphorylation and inactivation, which is essential for their anti-cancer therapeutic effect (Fig. 7f). Hence, the inhibition of HMG-CoA reductase by AT may be an effective strategy for the inhibition of MYC in the treatment and prevention of HCC.

Importantly, we confirmed the anti-tumor effects of statins that we observed both *in vitro* and *in vivo* were specific to HMG CoA reductase because they could be readily reversed by co-treatment with MV. We note that the AT doses we used in mice appear to be higher than generally used in humans. However, it is well known that, because of differences in the pharmacokinetics, murine doses have to be 50-fold higher than in humans (35,36). Moreover, we confirmed that the anti-tumor dose of AT did not exhibit *in vivo* toxicity (Fig. S4) and hence is likely to be achievable in humans.

The inhibition of HMG-CoA reductase was found to block MYC phosphorylation. First, AT treatment blocks MYC phosphorylation in murine and human HCC cells both *in vitro* and *in vivo*. Concomitant treatment with MV abrogates the ability of AT to block MYC phosphorylation and activation and mediate its suppressive effect on HCC growth, indicating that the anti-neoplastic effect of AT is *via* the inhibition of HMG-CoA reductase (Fig. 4). Second, a novel phosphorylation sensor was used to demonstrate *in situ* in human HCC cells and *in vivo* in living mice (Fig. 5). This phospho-sensor may be a useful approach to develop therapies that target MYC phosphorylation. Third, mutations in two MYC phosphorylation sites, specifically S62 and T58, blocks the ability of AT to inhibit tumor growth *in vivo*. Therefore, HMG-CoA reductase activity is important to the regulation of MYC phosphorylation.

We infer that MYC phosphorylation is an essential component of the mechanism by which statins mediate their anti-neoplastic properties. The introduction of mutant MYC alleles in HCC tumor cells reduced their sensitivity to statins *in vitro* and *in vivo*. Specifically, the differential ability of S62A and T58A MYC to block the effect of AT *in vitro* and *in vivo* (Fig. 6) suggests that AT-mediated reduction in phospho-S62 would therefore result in MYC phosphorylated at only T58, which is rapidly degraded in a ubiquitin-dependent manner (12,13). Our results are consistent with a role of S62 and T58 phosphorylation in MYC stability and transcriptional activity and, most importantly, their role in tumorigenesis (12). However, we note that S62/T58 phosphorylation has not always been found to regulate MYC stability (40). We conclude that the inhibition of MYC phosphorylation may be important to the mechanism by which the inhibition of HMG-CoA reductase by statins exerts its anti-neoplastic properties.

Many reports suggest that statins have anti-neoplastic properties (25,41–44). Many mechanisms have been proposed including: the inhibition of the ErbB2 pathway (45), the blocking of the interaction between the lymphocyte function-associated antigen (LFA) and intercellular cell adhesion molecule-1 (ICAM-1) (46), the suppression of geranylgeranylation of the Rho family proteins (47), and the prevention of the prenylation of RhoA and downstream activation of focal adhesion kinase, AKT, and beta-catenin (23). Although we cannot preclude any of these possibilities, our results are consistent with the notion that the inhibition of HMG-CoA reductase by AT in HCC cells blocks MYC phosphorylation likely through the inhibition of small GTPases in the Rac pathway (Fig. 7).

Our results are the first to suggest that HMG-CoA reductase regulates MYC activation *via* Rac. We are currently investigating the signaling intermediates that may function between Rac and MYC to mediate the anti-neoplastic effect of AT. Previously, it has been suggested that Rac regulates MYC (28). Rac1 can inhibit protein phosphatase PP2A (48), which has been shown to dephosphorylate MYC at S62 (13). One possible mechanism suggested by our work is that AT inhibition of Rac can result in activation of PP2A, which subsequently dephosphorylates MYC at S62 and induces the ubiquitin-dependent degradation of T58-phosphorylated MYC (Fig. 7f).

Our results illustrate that the inhibition of HMG-CoA reductase by statins may be useful in the treatment and prevention of human HCC. HCC is increasing in incidence, has a generally dismal prognosis, and there are few treatment options (49). Statins were developed to inhibit HMG-CoA reductase in the liver to reduce cholesterol. Hence, they may be aptly suited for treating cancers of the liver. Moreover, statins are well tolerated in humans and may be useful in the prevention of HCC in patients at high risk (49). Notably, some clinical studies have suggested that that the statin, pravastatin, may have clinical activity in patients with HCC (50,51), while other studies have not found clinical benefit (52). A possible explanation for this possible discrepancy in the benefit from statins is that clinical activity could depend upon the activation status of MYC. Also, AT may be a more effective statin for the treatment of HCC.

We conclude that MYC phosphorylation is a critical mechanism by which the inhibition of HMG-CoA Reductase by statins mediates their anti-neoplastic effects. We have shown that a novel molecular imaging sensor may be useful for the identification through high-throughput methods of new therapeutic agents that inhibit MYC phosphorylation and activation. Importantly, statins may be effective agents to inhibit MYC function as a treatment for HCC.

Supplementary Material

Refer to Web version on PubMed Central for supplementary material.

Acknowledgments

We would like to dedicate this paper in memory of Julie Do. We would like to thank Dr Rosalie C. Sears (Oregon Health & Science University, Portland, OR) for kindly providing us with mutant Myc constructs. We also value the helpful comments provided by Dr. Stacey Adam and the members of the Felsher, Sylvester, and Gambhir laboratories.

Financial Support: This work was supported by National Institutes of Health grants CA89305–01A1, CA89305–0351, CA105102, and CA112973; Department of Defense grant PR080163, the Burroughs Wellcome Fund; the Leukemia and Lymphoma Society; the Damon Runyon Foundation (D.W.F.); the *in vivo* cancer molecular image center (ICMIC P50) at Stanford grant CA114747 (S.S.G, D.W.F.). Dr. Zhongwei Cao was supported by an American Liver Foundation (A.L.F.) fellowship. Dr. Hua-Fan Minogue is supported by a NIH R25T training grant. Dr. David I. Bellovin is supported by the NIH under NRSA fellowship F32-CA132312.

References

1. Farazi PA, DePinho RA. Hepatocellular carcinoma pathogenesis: from genes to environment. Nat Rev Cancer. 2006; 6:674–87. [PubMed: 16929323]
2. Fausto N, Campbell JS, Riehle KJ. Liver regeneration. Hepatology. 2006; 43:S45–53. [PubMed: 16447274]
3. Riehle KJ, Campbell JS, McMahan RS, et al. Regulation of liver regeneration and hepatocarcinogenesis by suppressor of cytokine signaling 3. J Exp Med. 2008; 205:91–103. [PubMed: 18158318]
4. Coleman WB. Mechanisms of human hepatocarcinogenesis. Curr Mol Med. 2003; 3:573–88. [PubMed: 14527088]
5. Lee JS, Chu IS, Mikaelyan A, et al. Application of comparative functional genomics to identify best-fit mouse models to study human cancer. Nat Genet. 2004; 36:1306–11. [PubMed: 15565109]
6. Thorgeirsson SS, Factor VM, Snyderwine EG. Transgenic mouse models in carcinogenesis research and testing. Toxicology letters. 2000; 112–113:553–5.
7. Shachaf CM, Kopelman AM, Arvanitis C, et al. MYC inactivation uncovers pluripotent differentiation and tumour dormancy in hepatocellular cancer. Nature. 2004; 431:1112–7. [PubMed: 15475948]

8. Adhikary S, Eilers M. Transcriptional regulation and transformation by Myc proteins. Nat Rev Mol Cell Biol. 2005; 6:635–45. [PubMed: 16064138]
9. Kaposi-Novak P, Libbrecht L, Woo HG, et al. Central role of c-Myc during malignant conversion in human hepatocarcinogenesis. Cancer Res. 2009; 69:2775–82. [PubMed: 19276364]
10. Salghetti SE, Kim SY, Tansey WP. Destruction of Myc by ubiquitin-mediated proteolysis: cancer-associated and transforming mutations stabilize Myc. EMBO J. 1999; 18:717–26. [PubMed: 9927431]
11. Gregory MA, Qi Y, Hann SR. Phosphorylation by glycogen synthase kinase-3 controls c-myc proteolysis and subnuclear localization. J Biol Chem. 2003; 278:51606–12. [PubMed: 14563837]
12. Sears R, Nuckolls F, Haura E, Taya Y, Tamai K, Nevins JR. Multiple Ras-dependent phosphorylation pathways regulate Myc protein stability. Genes Dev. 2000; 14:2501–14. [PubMed: 11018017]
13. Yeh E, Cunningham M, Arnold H, et al. A signalling pathway controlling c-Myc degradation that impacts oncogenic transformation of human cells. Nat Cell Biol. 2004; 6:308–18. [PubMed: 15048125]
14. Bhatia K, Huppi K, Spangler G, Siwarski D, Iyer R, Magrath I. Point mutations in the c-Myc transactivation domain are common in Burkitt's lymphoma and mouse plasmacytomas. Nat Genet. 1993; 5:56–61. [PubMed: 8220424]
15. Smith-Sorensen B, Hijmans EM, Beijersbergen RL, Bernards R. Functional analysis of Burkitt's lymphoma mutant c-Myc proteins. J Biol Chem. 1996; 271:5513–8. [PubMed: 8621409]
16. Demierre MF, Higgins PD, Gruber SB, Hawk E, Lippman SM. Statins and cancer prevention. Nat Rev Cancer. 2005; 5:930–42. [PubMed: 16341084]
17. Shibata MA, Ito Y, Morimoto J, Otsuki Y. Lovastatin inhibits tumor growth and lung metastasis in mouse mammary carcinoma model: a p53-independent mitochondrial-mediated apoptotic mechanism. Carcinogenesis. 2004; 25:1887–98. [PubMed: 15180944]
18. Feleszko W, Mlynarczuk I, Balkowiec-Iskra EZ, et al. Lovastatin potentiates antitumor activity and attenuates cardiotoxicity of doxorubicin in three tumor models in mice. Clin Cancer Res. 2000; 6:2044–52. [PubMed: 10815931]
19. Goldstein JL, Brown MS. Regulation of the mevalonate pathway. Nature. 1990; 343:425–30. [PubMed: 1967820]
20. Wong WW, Dimitroulakos J, Minden MD, Penn LZ. HMG-CoA reductase inhibitors and the malignant cell: the statin family of drugs as triggers of tumor-specific apoptosis. Leukemia. 2002; 16:508–19. [PubMed: 11960327]
21. Narisawa T, Morotomi M, Fukaura Y, Hasebe M, Ito M, Aizawa R. Chemoprevention by pravastatin, a 3-hydroxy-3-methylglutaryl-coenzyme A reductase inhibitor, of N-methyl-N-nitrosourea-induced colon carcinogenesis in F344 rats. Jpn J Cancer Res. 1996; 87:798–804. [PubMed: 8797885]
22. Agarwal B, Rao CV, Bhendwal S, et al. Lovastatin augments sulindac-induced apoptosis in colon cancer cells and potentiates chemopreventive effects of sulindac. Gastroenterology. 1999; 117:838–47. [PubMed: 10500066]
23. Denoyelle C, Albanese P, Uzan G, et al. Molecular mechanism of the anti-cancer activity of cerivastatin, an inhibitor of HMG-CoA reductase, on aggressive human breast cancer cells. Cell Signal. 2003; 15:327–38. [PubMed: 12531431]
24. He L, Mo H, Hadisusilo S, Qureshi AA, Elson CE. Isoprenoids suppress the growth of murine B16 melanomas in vitro and in vivo. J Nutr. 1997; 127:668–74. [PubMed: 9164984]
25. Shachaf CM, Perez OD, Youssef S, et al. Inhibition of HMGcoA reductase by atorvastatin prevents and reverses MYC-induced lymphomagenesis. Blood. 2007; 110:2674–84. [PubMed: 17622571]
26. Hindler K, Cleeland CS, Rivera E, Collard CD. The role of statins in cancer therapy. Oncologist. 2006; 11:306–15. [PubMed: 16549815]
27. Jackson SM, Ericsson J, Edwards PA. Signaling molecules derived from the cholesterol biosynthetic pathway. Subcell Biochem. 1997; 28:1–21. [PubMed: 9090289]
28. Chiariello M, Marinissen MJ, Gutkind JS. Regulation of c-myc expression by PDGF through Rho GTPases. Nat Cell Biol. 2001; 3:580–6. [PubMed: 11389443]

29. Mesri M, Wall NR, Li J, Kim RW, Altieri DC. Cancer gene therapy using a survivin mutant adenovirus. J Clin Invest. 2001; 108:981–90. [PubMed: 11581299]
30. Paulmurugan R, Gambhir SS. Monitoring protein-protein interactions using split synthetic renilla luciferase protein-fragment-assisted complementation. Anal Chem. 2003; 75:1584–9. [PubMed: 12705589]
31. Fan-Minogue H, Cao Z, Paulmurugan R, et al. Noninvasive molecular imaging of c-Myc activation in living mice. Proc Natl Acad Sci U S A. 107:15892–7. [PubMed: 20713710]
32. Liu F, Song Y, Liu D. Hydrodynamics-based transfection in animals by systemic administration of plasmid DNA. Gene Ther. 1999; 6:1258–66. [PubMed: 10455434]
33. Black AE, Sinz MW, Hayes RN, Woolf TF. Metabolism and excretion studies in mouse after single and multiple oral doses of the 3-hydroxy-3-methylglutaryl-CoA reductase inhibitor atorvastatin. Drug Metab Dispos. 1998; 26:755–63. [PubMed: 9698289]
34. Lubet RA, Boring D, Steele VE, Ruppert JM, Juliana MM, Grubbs CJ. Lack of efficacy of the statins atorvastatin and lovastatin in rodent mammary carcinogenesis. Cancer Prev Res (Phila). 2009; 2:161–7. [PubMed: 19196723]
35. Pinkel D. The use of body surface area as a criterion of drug dosage in cancer chemotherapy. Cancer Res. 1958; 18:853–6. [PubMed: 13573353]
36. Reagan-Shaw S, Nihal M, Ahmad N. Dose translation from animal to human studies revisited. FASEB J. 2008; 22:659–61. [PubMed: 17942826]
37. Lutterbach B, Hann SR. Hierarchical phosphorylation at N-terminal transformation-sensitive sites in c-Myc protein is regulated by mitogens and in mitosis. Mol Cell Biol. 1994; 14:5510–22. [PubMed: 8035827]
38. Denoyelle C, Vasse M, Korner M, et al. Cerivastatin, an inhibitor of HMG-CoA reductase, inhibits the signaling pathways involved in the invasiveness and metastatic properties of highly invasive breast cancer cell lines: an in vitro study. Carcinogenesis. 2001; 22:1139–48. [PubMed: 11470741]
39. Jakobisiak M, Bruno S, Skierski JS, Darzynkiewicz Z. Cell cycle-specific effects of lovastatin. Proc Natl Acad Sci U S A. 1991; 88:3628–32. [PubMed: 1673788]
40. Henriksson M, Bakardjiev A, Klein G, Luscher B. Phosphorylation sites mapping in the N-terminal domain of c-myc modulate its transforming potential. Oncogene. 1993; 8:3199–209. [PubMed: 8247524]
41. Gniadecki R. Depletion of membrane cholesterol causes ligand-independent activation of Fas and apoptosis. Biochem Biophys Res Commun. 2004; 320:165–9. [PubMed: 15207716]
42. Kureishi Y, Luo Z, Shiojima I, et al. The HMG-CoA reductase inhibitor simvastatin activates the protein kinase Akt and promotes angiogenesis in normocholesterolemic animals. Nat Med. 2000; 6:1004–10. [PubMed: 10973320]
43. Weis M, Heeschen C, Glassford AJ, Cooke JP. Statins have biphasic effects on angiogenesis. Circulation. 2002; 105:739–45. [PubMed: 11839631]
44. Tilkin-Mariame AF, Cormary C, Ferro N, et al. Geranylgeranyl transferase inhibition stimulates anti-melanoma immune response through MHC Class I and costimulatory molecule expression. FASEB J. 2005; 19:1513–5. [PubMed: 15990392]
45. Mueck AO, Seeger H, Wallwiener D. Effect of statins combined with estradiol on the proliferation of human receptor-positive and receptor-negative breast cancer cells. Menopause. 2003; 10:332–6. [PubMed: 12851516]
46. Chan KK, Oza AM, Siu LL. The statins as anticancer agents. Clin Cancer Res. 2003; 9:10–9. [PubMed: 12538446]
47. Agarwal B, Halmos B, Feoktistov AS, et al. Mechanism of lovastatin-induced apoptosis in intestinal epithelial cells. Carcinogenesis. 2002; 23:521–8. [PubMed: 11895868]
48. ten Klooster JP, Leeuwen I, Scheres N, Anthony EC, Hordijk PL. Rac1-induced cell migration requires membrane recruitment of the nuclear oncogene SET. EMBO J. 2007; 26:336–45. [PubMed: 17245428]
49. Altekruse SF, McGlynn KA, Reichman ME. Hepatocellular Carcinoma Incidence, Mortality, and Survival Trends in the United States From 1975 to 2005. J Clin Oncol. 2009

50. Graf H, Jungst C, Straub G, et al. Chemoembolization combined with pravastatin improves survival in patients with hepatocellular carcinoma. Digestion. 2008; 78:34–8. [PubMed: 18797167]

51. Kawata S, Yamasaki E, Nagase T, et al. Effect of pravastatin on survival in patients with advanced hepatocellular carcinoma. A randomized controlled trial. Br J Cancer. 2001; 84:886–91. [PubMed: 11286466]

52. Lersch C, Schmelz R, Erdmann J, et al. Treatment of HCC with pravastatin, octreotide, or gemcitabine--a critical evaluation. Hepatogastroenterology. 2004; 51:1099–103. [PubMed: 15239254]

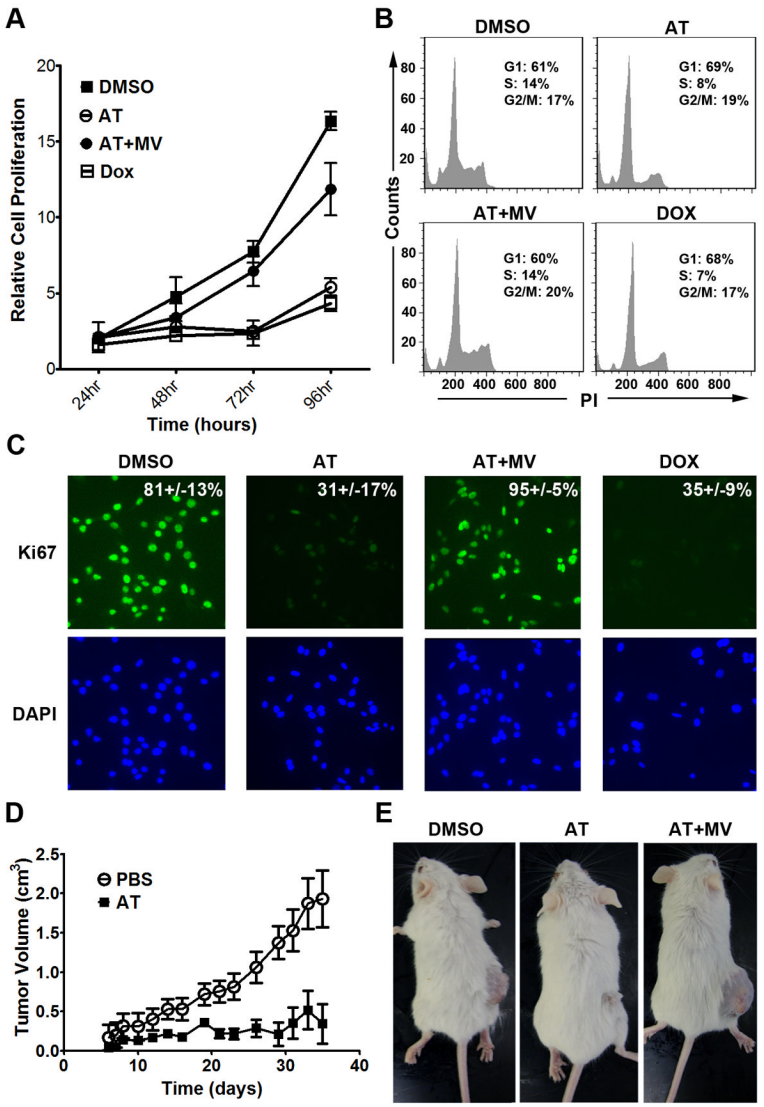

Figure 1. Inhibition of HMG-CoA reductase by atorvastatin (AT) suppresses growth of MYC-induced hepatocellular carcinoma (HCC) *in vitro* and *in vivo*

a) AT inhibits the proliferation of a MYC-induced HCC tumor derived cell line, 3–4. MTT assay was performed every 24 hours for 4 days on HCC cells treated with 10μM AT, AT plus 100μM MV, or DMSO as a vehicle control. Cells were also treated with doxycycline (Dox) to inactivate transgenic MYC as a positive control. All experiments were repeated 3 times ($p<0.0001$). Error bars represent standard deviation. **b)** AT induces cell cycle arrest in murine HCC as assessed by FACS analysis of PI stained cells ($p=0.01$). Cells were treated with 10μM AT, AT plus MV, DMSO, or Dox for 48 hr. **c)** Immunofluorescence for Ki67 on HCC cells treated with 10μM AT for 48hr demonstrates that statin treatment inhibits HCC proliferation ($p<0.0001$). **d)** AT inhibits growth of MYC-induced HCC cells *in vivo*. Murine HCC cells were subcutaneously transplanted into FVB/N mice treated with PBS (n=5) or AT (n=5). $p=0.0003$. Error bars represent standard deviation. **e)** Representative images of mice treated with PBS (left), AT (middle), or AT plus MV (right) shows that AT suppresses growth of MYC-induced HCC *in vivo*.

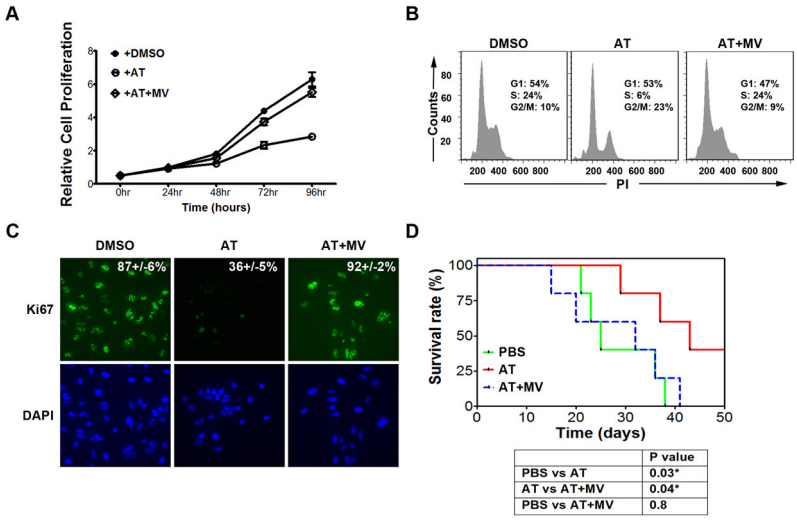

Figure 2. Blocking HMG-CoA reductase via AT inhibits growth of human HCC cells *in vitro* and *in vivo*

a) MTT analysis of the human HCC cell line, Huh7, treated with 10μM AT demonstrates significant inhibition of growth *in vitro* ($p<0.0001$). Error bars represent standard deviation. **b)** FACS analysis of PI-stained Huh7 cells reveals that AT suppresses cell cycle progression ($p=0.0003$). Cells were treated with 10μM AT for 48hr. **c)** Huh7 cells treated with 10μM AT for 48hr were examined by immunofluorescence for Ki67, demonstrating statin-induced reduction in proliferative cells ($p<0.0001$). **d)** Huh7 cells were transplanted intraperitoneally into SCID mice, and host animals were treated with PBS, AT, or AT with MV. A Kaplan-Meier curve demonstrates a significant increase in survival of animals treated with AT (PBS *versus* AT, $p=0.03$; AT *versus* AT+MV, $p=0.04$; PBS *versus* AT+MV, $p=0.8$).

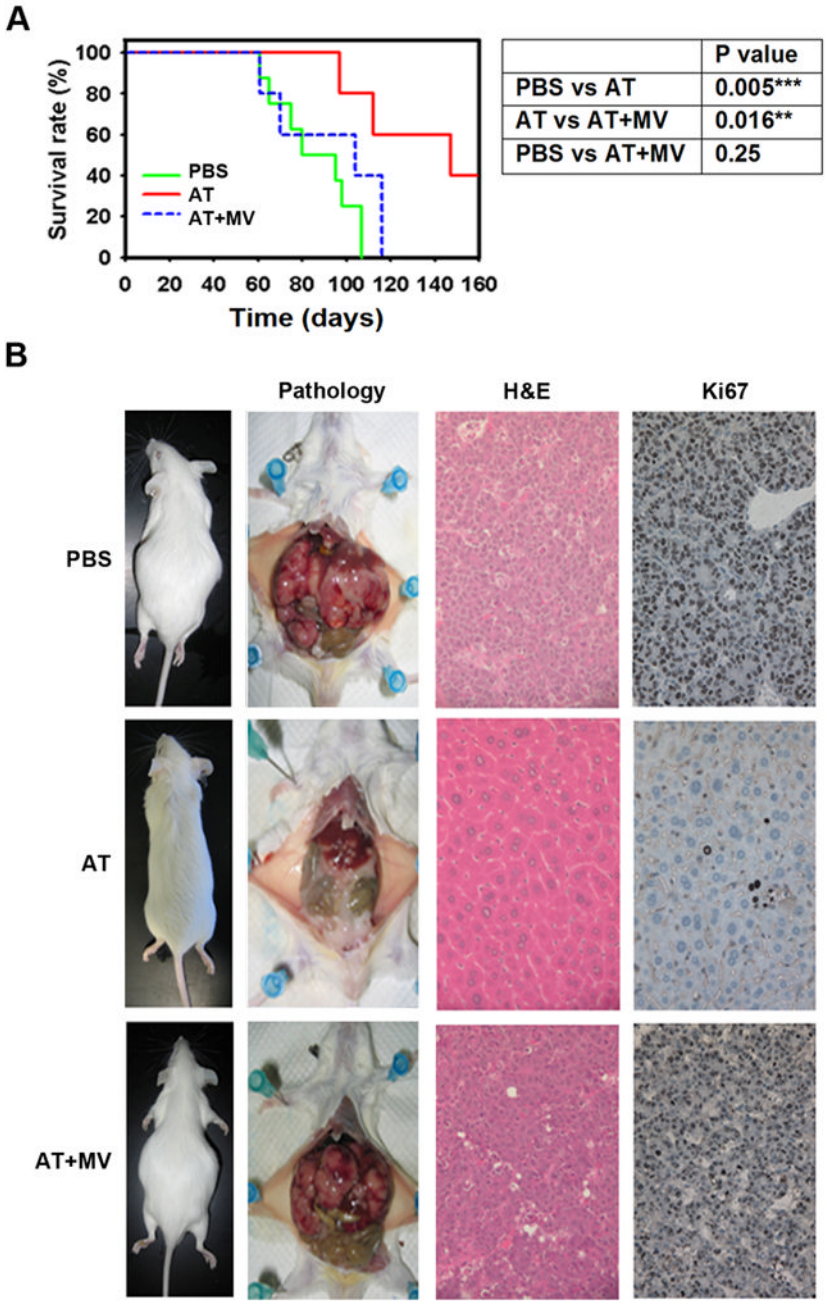

	P value
PBS vs AT	0.005***
AT vs AT+MV	0.016**
PBS vs AT+MV	0.25

Figure 3. AT inhibition of HMG-CoA reductase suppresses MYC-induced hepatocellular tumorigenesis

a) Kaplan-Meier survival curves of adult LAP-tTA/TRE-MYC mice treated with PBS (n=8), 100mg/kg AT (n=5), or AT with MV (n=5) three times per week demonstrates a significant increase in survival of animals treated with AT (PBS *versus* AT, p=0.005; AT *versus* AT/MV, p=0.016; PBS *versus* AT/MV, p=0.25). **b)** Representative pictures from each treatment group are shown. Gross anatomy reveals inhibition of tumor onset due to AT treatment. H&E staining shows that normal hepatic structure is maintained by AT treatment (middle row), which was reversed by MV treatment (bottom row). Immunohistochemistry for Ki67 shows a significant inhibition of proliferation due to AT (right column, 8 ± 3 positive cells *versus* 422 ± 23 positive cells per high power field; p<0.02).

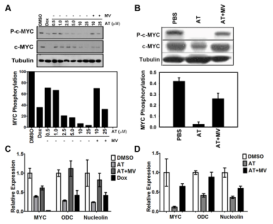

Figure 4. Inhibition of HMG-CoA reductase blocks MYC activity by reducing its phosphorylation

a) Murine HCC cells were treated with indicated concentrations of AT with or without MV for 24 hours. MYC phosphorylation and expression are suppressed by AT treatment in a dose-dependent manner (p=0.002). Values are normalized to the DMSO control. Representative immunoblots are shown. **b)** Primary liver tissue of transgenic animals shows an AT-dependent suppression of MYC phosphorylation (p=0.04). Representative immunoblots are shown. Error bars represent standard deviation. **c)** qPCR analysis of MYC and MYC target gene mRNA expression in murine HCC cells. Treatment of cells with 10μM AT for 24 hours results in reduced MYC transcriptional activity as shown by 72% and 76% reduction in expression of ODC and nucleolin, respectively (p=0.003, p=0.03). Expression is normalized to ubiquitin and values are relative to DMSO control. Error bars represent standard deviation. **d)** qPCR analysis of MYC and MYC target gene mRNA expression in human Huh7 cells. Cells were treated with 10μM AT for 24hr and demonstrate suppression of MYC transcriptional activity as assessed by reductions of 64% for ODC and 59% for nucleolin expression (p=0.016, p=0.008). Expression is normalized to ubiquitin and values are relative to DMSO control. Error bars represent standard deviation.

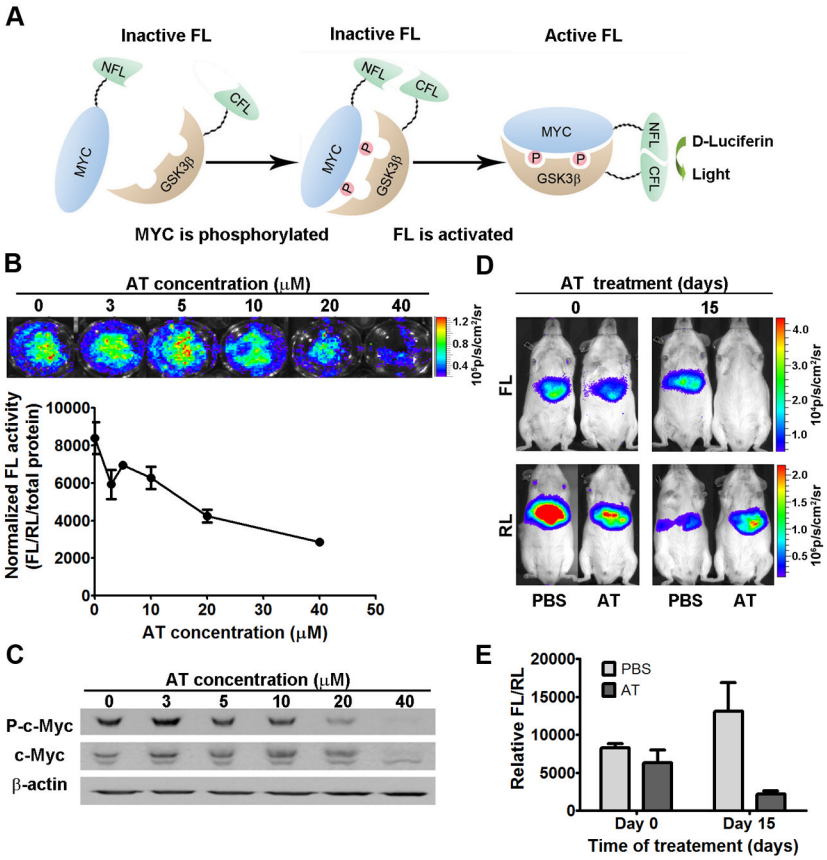

Figure 5. A novel bioluminescence c-Myc phospho-sensor noninvasively demonstrates AT-dependent inhibition of MYC phosphorylation

a) The N- and C-termini of split firefly luciferase (FL) were fused to the phospho-regulated domain of c- Myc and the corresponding domain of GSK3β, respectively. Phosphorylation of the c- Myc peptide results in FL enzymatic activity. **b**) Huh7 cells were transfected with the c-Myc phosphorylation sensor and treated with AT. Bioluminescent imaging (BLI) shows a dose-dependent inhibition of phospho-MYC (*p<0.0001*). Firefly luciferase (FL) activity was normalized to Renilla luciferase (RL) activity and plotted against AT concentration. Error bars represent standard deviation. **c)** Western blot analysis confirms AT-dependent suppression of phospho-c-Myc in transfected Huh7 cells. **d)** LAP-tTA/TRE-MYC transgenic mice were treated with AT or PBS (n=3), and hydrodynamic injection of the phospho-sensor followed by BLI shows AT-dependent inhibition of c-Myc phosphorylation *in vivo* (AT-treated mice day 0 *versus* day 15, *p=0.038*; PBS-treated mice day 0 *versus* day 15, *p=0.638*). **e)** FL activity was normalized to RL activity and plotted against days of AT treatment.

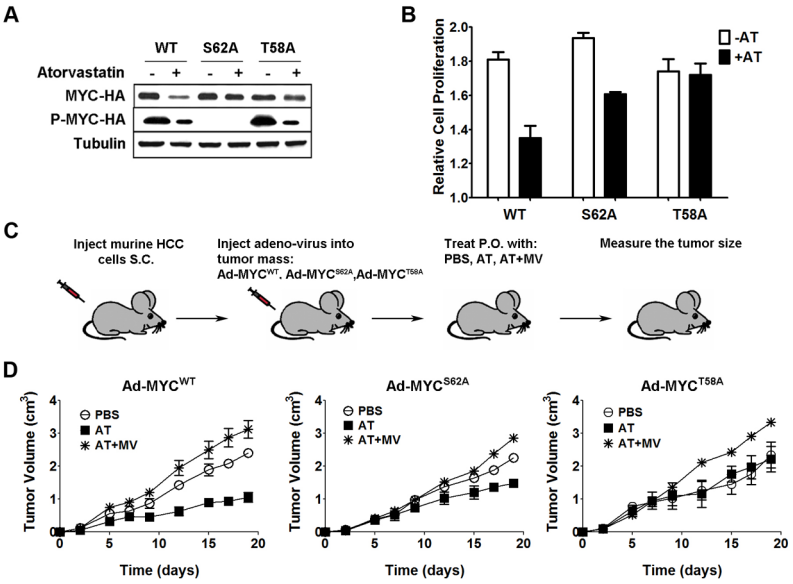

Figure 6. HCC transduced with S62A or T58A MYC phospho-mutants demonstrate reduced sensitivity to HMG-CoA reductase inhibition

a) Murine HCC cells were infected with Ad-MYC^{WT} (WT), Ad-MYC^{S62A} (S62A), or Ad-MYC^{T58A} (T58A) adenovirus, and HA-tagged MYC was immunoprecipitated using an antibody to the HA tag. Immunoblot analysis suggests that AT-dependent phospho-regulation of MYC is via S62. However, the inhibition of protein stability requires both S62 and T58 phospho- regulation. Cells were treated with 10μM AT for 24 hr. **b)** S62A partially and T58A completely abrogated AT inhibition of cell proliferation (S62A: PBS *versus* AT, $p<0.0001$; T58A: PBS *versus* AT $p=0.8$). Error bars represent standard deviation. **c)** HCC cells isolated from transgenic animals were transplanted into SCID mice, injected with Ad-MYC^{WT}, Ad-MYC^{S62A}, or Ad-MYC^{T58A} once every week, and orally treated with PBS (n=6), AT (n=5), or AT with MV (n=5) together with Dox. Tumor growth was measured three times per week. **d)** *In vivo* growth kinetics of HCC infected with Ad-MYC^{WT} show that AT inhibits tumor growth *in vivo* (Left, PBS *versus* AT, $p=0.01$; AT *versus* AT+MV, $p=0.007$). Error bars represent standard deviation. Infection with Ad-MYC^{S62A} partially rescues growth inhibition due to AT (Middle, PBS *versus* AT, $p=0.02$; AT *versus* AT+MV, $p=0.03$). Error bars represent standard deviation. Ad-MYC^{T58A} completely rescues AT-mediated growth inhibition of HCC (Right, PBS *versus* AT, $p=0.56$; AT *versus* AT+MV, $p=0.03$). Error bars represent standard deviation.

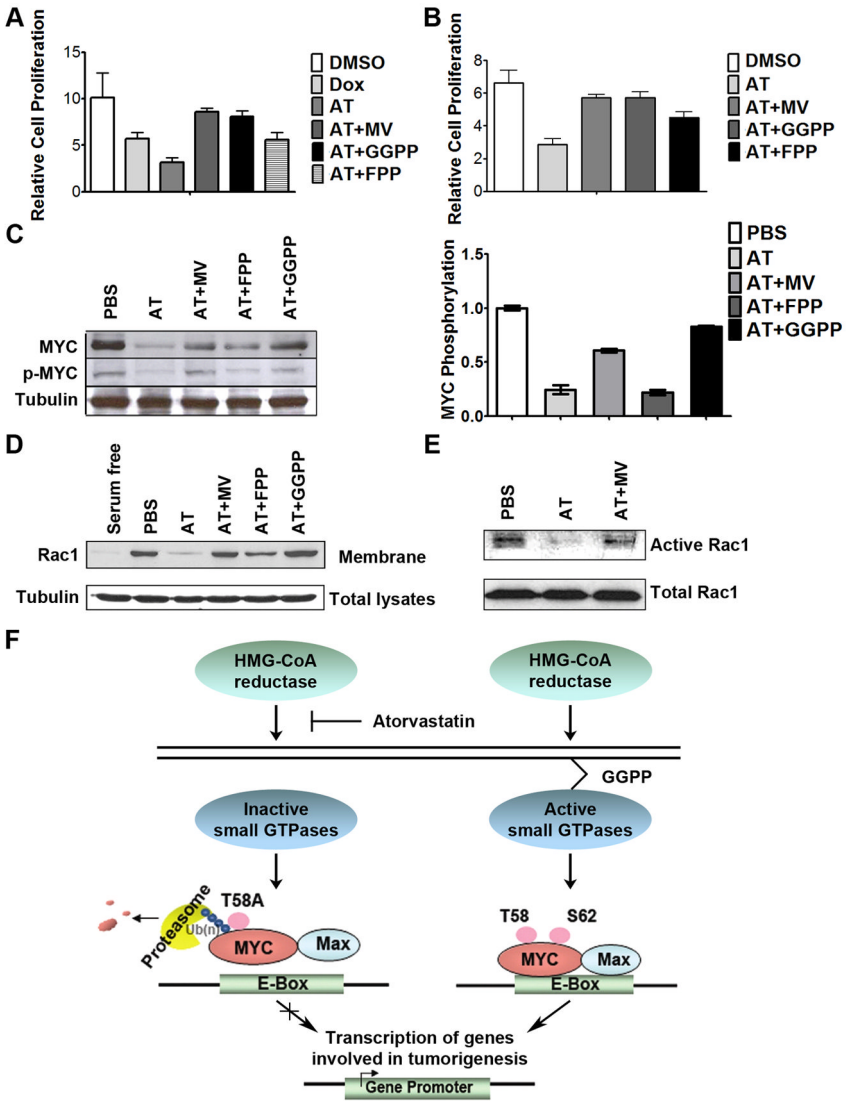

Figure 7. HMG-CoA reductase influences MYC phosphorylation through a Rac GTPase-dependent mechanism

a) Suppression of murine HCC growth *in vitro* upon 10μM AT treatment for 96 hours is rescued by GGPP treatment, as assessed by MTT (DMSO *versus* AT+MV, p=0.07; DMSO *versus* GGPP, p=0.053, DMSO *versus* FPP, p=0.002). Error bars represent standard deviation. **b)** GGPP treatment rescues the AT- dependent suppression in human HCC cell growth upon 10μM AT treatment (DMSO *versus* AT+MV, p=0.01; DMSO *versus* GGPP, p=0.01, DMSO *versus* FPP, p<0.001). Error bars represent standard deviation. **c)** GGPP treatment rescues AT-dependent inhibition of MYC phosphorylation. Representative immunoblots are shown. Error bars represent standard deviation. **d)** GGPP treatment prevents the decrease in the membrane accumulation of Rac induced by 24 hours of 10μM AT. **e)** AT treatment inhibits Rac activity. Rac activity was reduced by 77% as measured by pull-down assay. **f)** Our results suggest a model in which inhibition of HMG-CoA reductase by AT blocks prenylation and activation of small GTPases, specifically including Rac. AT-mediated inhibition of Rac likely results in reduction of phospho-S62 MYC. Dephosphorylation at S62 in the context of phospho-T58 thereby results in the ubiquitin-

mediated degradation of MYC. As such, AT treatment ultimately results in the inhibition of MYC oncogenic activity and suppressed hepatocellular carcinogenesis.